Cancer Research

The Myc–miR-17~92 Axis Blunts TGFβ Signaling and Production of Multiple TGFβ-Dependent Antiangiogenic Factors

Michael Dews[1], Jamie L. Fox[1,2], Stacy Hultine[1], Prema Sundaram[1], Wenge Wang[3], Yingqiu Y. Liu[3], Emma Furth[3], Gregory H. Enders[2,3], Wafik El-Deiry[2,3], Janell M. Schelter[4], Michele A. Cleary[4], and Andrei Thomas-Tikhonenko[1,2,3]

Abstract

c-Myc stimulates angiogenesis in tumors through mechanisms that remain incompletely understood. Recent work indicates that c-Myc upregulates the miR-17~92 microRNA cluster and downregulates the angiogenesis inhibitor thrombospondin-1, along with other members of the thrombospondin type 1 repeat superfamily. Here, we show that downregulation of the thrombospondin type 1 repeat protein clusterin in cells overexpressing c-Myc and miR-17~92 promotes angiogenesis and tumor growth. However, clusterin downregulation by miR-17~92 is indirect. It occurs as a result of reduced transforming growth factor-β (TGFβ) signaling caused by targeting of several regulatory components in this signaling pathway. Specifically, miR-17-5p and miR-20 reduce the expression of the type II TGFβ receptor and miR-18 limits the expression of Smad4. Supporting these results, in human cancer cell lines, levels of the miR-17~92 primary transcript MIR17HG negatively correlate with those of many TGFβ-induced genes that are not direct targets of miR-17~92 (e.g., clusterin and angiopoietin-like 4). Furthermore, enforced expression of miR-17~92 in MIR17HG^{low} cell lines (e.g., glioblastoma) results in impaired gene activation by TGFβ. Together, our results define a pathway in which c-Myc activation of miR-17~92 attenuates the TGFβ signaling pathway to shut down clusterin expression, thereby stimulating angiogenesis and tumor cell growth. *Cancer Res; 70(20); 8233–46. ©2010 AACR.*

Introduction

Although the c-Myc proto-oncogene is generally thought to control cell proliferation, apoptosis, and differentiation, its contribution to non–cell-autonomous cancer phenotypes such as angiogenesis (formation of new blood vessels) has only recently come to the fore (1, 2). The propensity of Myc to induce the angiogenic phenotype was observed in several models, including mouse papillomatosis (3, 4), chicken bursal lymphomagenesis (5), and Rat-1A cell xenografts (6). However, molecular events triggering the angiogenic switch in Myc-transformed cells remained incompletely understood.

To identify Myc-regulated angiogenic factors, we developed an experimental system wherein overexpression of this oncoprotein in murine colon carcinoma cells resulted in the hypervascular phenotype. This occurred without increased production of vascular endothelial growth factor. Instead, Myc downregulated the potent endogenous inhibitor of angiogenesis thrombospondin-1 as well as several other thrombospondin type I repeat (TSR) proteins, such as connective tissue growth factor (CTGF) and clusterin (7). Thrombospondin-1 is downregulated primarily at the level of mRNA turnover (8), suggesting the involvement of microRNAs, which are known to contribute to mRNA degradation (9). Several Myc-regulated microRNAs are known to be important for Myc-induced phenotypes (10, 11) and, provocatively, Myc has been reported to upregulate the miR-17~92 microRNA cluster (12), the predicted targets of which include thrombospondin-1 and other TSR proteins.

Our published results confirmed that miR-17~92 controls TSR protein levels. Moreover, overexpression of miR-17~92 in murine carcinoma cells mimicked cell-extrinsic effects of Myc and resulted in enhanced tumor angiogenesis (7). However, it remained unclear whether nonthrombospondin members of the TSR superfamily (such as clusterin) also

Authors' Affiliations: [1]Division of Cancer Pathobiology, Department of Pathology and Laboratory Medicine, The Children's Hospital of Philadelphia Research Institute, [2]Cancer Biology Program, Cell and Molecular Biology Graduate Group, [3]School of Medicine, University of Pennsylvania, Philadelphia, Pennsylvania; and [4]Rosetta Inpharmatics, Seattle, Washington

Note: J. Fox and S. Hultine contributed equally to this work.

Present address for G.H. Enders: Department of Medicine, Fox Chase Cancer Center, 333 Cottman Avenue, Philadelphia, PA 19111-2497.

Present address for W. Wang, Y.Y. Liu, and W. El-Deiry: Penn State Hershey Cancer Institute, 500 University Drive, Hershey, PA 17033.

Present address for J.M. Schelter and M.A. Cleary: Department of Automated Biotechnology, Merck & Co., Inc., 502 Louise Lane, North Wales, PA 19454.

Corresponding Author: Andrei Thomas-Tikhonenko, 4056 Colket Translational Research Building, 3501 Civic Center Boulevard, Philadelphia, PA 19104-4399. Phone: 267-426-9699; Fax: 267-426-8125; E-mail: andreit@mail.med.upenn.edu.

doi: 10.1158/0008-5472.CAN-10-2412

act to inhibit tumor angiogenesis and whether miR-17∼92 regulates them as well. In this report, we first focused on clusterin because our prior works had shown that clusterin inhibits neoplastic transformation of epithelial cells *in vivo* (13) and acts as a haploinsufficient tumor suppressor in the mouse model of neuroblastoma (14). However, its function during tumor progression is a matter of considerable controversy (15), as are the mechanisms of its downregulation by c-Myc. Our initial data suggested that clusterin is regulated by miR-17∼92, but indirectly, in a transforming growth factor-β (TGFβ)–dependent manner. This led us to explore the effects of Myc and miR-17∼92 on TGFβ signaling and discover that miR-17∼92 is a global attenuator of this important pathway.

Materials and Methods

Cell lines and tumor production

All cell lines were maintained in DMEM supplemented with 10% fetal bovine serum and antibiotics. Parental, K-Ras-, and K-Ras + Myc–transformed p53-null colonocytes were described previously (13, 16). HCT116 p53-null human colon carcinoma cells were a kind gift from Dr. Burt Vogelstein. To overexpress miR-17∼92 in Ras colonocytes, a *Bam*HI-*Eco*RV fragment containing miR-17∼92 (12) was excised from pcDNA3.1 and inserted into pRNA-CMV3.1/Puro (GenScript). Cells were transfected using LipofectAMINE 2000 and selected in puromycin. Human hepatocellular carcinoma and glioblastoma cell lines overexpressing miR-17∼92 were generated by infection with the MSCVpuro retrovirus containing miR-17∼92 as described previously (7). Murine clusterin was overexpressed in p53-null colonocytes using the MigR1 retrovirus. Ras-transformed colonocytes were transduced with the QCXIP (Clontech) retrovirus containing the mouse clusterin coding sequence and selected with puromycin. HCT116 cells were likewise transduced with QCXIP expressing human clusterin, and additionally, with a retrovirus expressing firefly luciferase.

Treatment of cells with microRNA inhibitors was as described previously (7). For most microRNA mimics experiments, HCT116 and DLD1 cells bearing a hypomorphic mutation in Dicer ($Dicer^{hypo}$; ref. 17) were used. MicroRNA mimics were purchased from Dharmacon and transfected using LipofectAMINE 2000 or HiPerfect (Qiagen) in the case of A172 cells. Short interfering RNA (siRNA) against the type II TGFβ receptor was purchased as a Smart Pool from Dharmacon and transfected into cells using LipofectAMINE RNAi Max (Invitrogen).

C57BL6/NCr mice were obtained from National Cancer Institute (Frederick, MD) and used as syngeneic hosts for murine colonocytes. Transformed colonocytes were implanted subcutaneously. Tumor sizes were measured using calipers and tumor weights were recorded on the day of tumor excision. For *in vivo* imaging of HCT116 xenografts, BALB/c nude mice (Charles River Laboratories) were inoculated s.c. with 2×10^6 cells resuspended in 50 μL of Matrigel. Optical imaging was done using the Xenogen In vivo Imaging System. For immunohistochemical analysis, unmodified HCT116 cells were grown subcutaneously in nonobese diabetic-severe combined immunodeficiency/NCr mice (National Cancer Institute).

Analyses of tumor specimens and blood vasculature

Following excision, tumor pieces were placed in embedding molds containing ornithine carbamyl transferase, snap-frozen, and stored at −80°C. Using a cryostat, 6-μm-thick sections were prepared and placed on glass slides. Slides were allowed to dry, and then stored at −80°C until use. Slides containing tumor sections were warmed to room temperature, fixed by placing in 10% formalin for 5 minutes, and then rinsed with 1× PBS for 10 minutes. To block endogenous peroxidase, the slides were immersed in 3% hydrogen peroxide for 15 minutes, and then rinsed with water for 5 minutes. Blocking of endogenous biotin was accomplished by using avidin/biotin blocking kit (Vector Labs, Inc.), and to reduce background staining, blocking was done using M.O.M. Basic Kit (Vector Labs) A biotinylated antibody against CD31 (MEC 7.46; Abcam, ab7389) was applied at a concentration of 1:50 and incubated for 1 hour at 37°C. Slides were rinsed three times for 5 minutes with 1× PBS. ABC immunoperoxidase detection kit (Vector Labs) was applied to slides and incubated for 30 minutes at 37°C. Slides were rinsed three times for 5 minutes with 1× PBS. Slides were then developed using 3,3′-diaminobenzidine substrate kit.

Digitalized slides of H&E– or α-CD31–stained tumors were analyzed to detect pixels that correspond to either RBC or CD31-positive endothelial cells and thus represent blood vessels. Aperio ImageScope (V10.0.36.1805) software, and the Positive Pixel Count algorithm (V9.1) were used for this purpose. The total numbers of positive and strong positive pixels were divided by the total area of the analyzed section (expressed as mm^2) to yield pixel density. Statistical significance was calculated using two-tailed Student's t test (for the counting of α-CD31–stained vessels) or two-tailed Mann-Whitney U test (for the counting of perfused vessels).

Staining for clusterin was done on formalin-fixed, paraffin-embedded tissue sections as described previously (18). Tumor cell proliferation was assayed by immunoperoxidase staining for Ki-67 in paraffin-embedded tissue sections using standard methods. The use of p53-null colonocytes for *in vivo* Matrigel assays has been described in detail previously (19).

Western blotting

Cells were lysed in radioimmunoprecipitation assay buffer containing phenylmethylsulfonyl fluoride and cocktails of protease (Sigma) and phosphatase (Pierce) inhibitors. Lysates were separated on SDS-PAGE mini-gels (Lonza) under reducing conditions and transferred to polyvinylidene difluoride membranes. For thrombospondin-1 expression analysis, either cell lysates or conditioned media were used. Membranes were probed with antibodies to clusterin, CTGF, TGFBR2 (Santa Cruz Biotechnology and Abcam), Smad4 (Santa Cruz Biotechnology), Smad2 and Smad3 (Invitrogen), phosphorylated Smad3 (Cell Signaling), and Tsp-1 (Ab-11, Lab Vision) according to the recommendations of the manufacturer. Conditioned media were loaded on PAGE neat. Appropriate secondary antibodies were used

in horseradish peroxidase–conjugated forms (Amersham Biosciences). Antibody binding was detected using the enhanced chemiluminescence system (Amersham) and Quantity One software (Bio-Rad). A monoclonal antibody reactive with actin (Sigma) was used to confirm equal loading.

Quantitation by Odyssey Infrared Imager

After transfer, the polyvinylidene difluoride membrane was incubated with 10 mL of LI-COR blocking buffer (LI-COR Biosciences) for 1 hour at room temperature with gentle agitation. To determine the ratios of Smad4 and TGFBRII levels to actin, the membrane was incubated simultaneously with the Smad4 antibody and actin antibody (1:500 and 1:500,000, respectively), or TGFBRII antibody and actin antibody (1:500 and 1:500,000, respectively) and incubated overnight at 4°C with gentle agitation. After incubation, the membrane was washed with TBS with 0.1% Tween (TBS-T) three times for 10 minutes each. The membrane was incubated with a fluorescently labeled antibody, either IRDye 680 donkey anti-mouse IgG and/or IRDye 800CW donkey anti-rabbit (1:10,000), in 10 mL of LI-COR blocking buffer with 0.1% Tween, for 1 hour at room temperature. After incubation, the membrane was washed with TBS-T three times for 10 minutes each. The wet membrane was analyzed on an Odyssey Infrared Imager (LI-COR Biosciences).

Luciferase reporter constructs and assays

To analyze the interaction of microRNAs with the human TGFBR2 and Smad4 genes, sense and antisense oligonucleotides encompassing approximately 100 bp surrounding the predicted microRNA binding sites were synthesized with ends compatible with *Xho*I and *Not*I. Annealed oligonucleotides were ligated downstream of the renilla luciferase gene in the psiCHECK-2 vector (Promega). DLD1Dicer^{hypo} cells were lysed 48 hours after transfection with reporter constructs, and ratios of firefly to renilla luciferase activities were measured using the dual luciferase assay (Promega). Luminescence was measured on a Synergy 2 luminometer (BioTek).

The sequences of TGFBR2 3′-untranslated region (UTR) oligonucleotides were as follows:

miR-17-5p WT sense: TCGAGCCTCAGGAAATGAGATTGATTTTTACAATAGCCAATAACATTTGCACTTTATTAATGCCTGTATATAAATATGAATAGCTATGTTTTATATATGC

miR-17-5p WT a/sense: GGCCGCATATATAAAACATAGCTATTCATATTTATATACAGGCATTAATAAAGTGCAAATGTTATTGGCTATTGTAAAAATCAATCTCATTTCCTGAGGC

miR-17-5p mut sense: TCGAGCCTCAGGAAATGAGATTGATTTTTACAATAGCCAATAACATTTACGCTGTATTAATGCCTGTATATAAATATGAATAGCTATGTTTTATATATGC

miR-17-5p mut a/sense: GGCCGCATATATAAAACATAGCTATTCATATTTATATACAGGCATTAATACAGCGTAAATGTTATTGGCTATTGTAAAAATCAATCTCATTTCCTGAGGC

The sequences of Smad4 3′-UTR oligonucleotides were as follows:

miR-17-5p WT sense: TCGAGCCTCAGGAAATGAGATTGATTTTTACAATAGCCAATAACATTTGCACTTTATTAATGCCTGTATATAAATATGAATAGCTATGTTTTATATATGC

miR-17-5p WT a/sense: GGCCGCCTGTCATTTAGTAGAAGGTACCTCATCACTGAGATTGGACTCAAAAGTGCAAAAGAAAAAAAAAATCTTAAAAATCAAACCTAGAATTCAACTC

miR-17-5p mut sense: TCGAGAGTTGAATTCTAGGTTTGATTTTTAAGATTTTTTTTTTCTTTTACAATTCTGAGTCCAATCTCAGTGATGAGGTACCTTCTACTAAATGACAGGC

miR-17-5p mut a/sense: GGCCGCCTGTCATTTAGTAGAAGGTACCTCATCACTGAGATTGGACTCAGAATTGTAAAAGAAAAAAAAAATCTTAAAAATCAAACCTAGAATTCAACTC

miR-18a WT sense: TCGAGATAGTATGCCCTTAAGACTTAATTTTAACCAAAGGCCTAGCACCACCTTAGGGGCTGCAATAAACACTTAACGCGCGTGCGCACGCGCGCGCGGC

miR-18a WT a/sense: GGCCGCCGCGCGCGCGTGCGCACGCGCGTTAAGTGTTTATTGCAGCCCCTAAGGTGGTGCTAGGCCTTTGGTTAAAATTAAGTCTTAAGGGCATACTATC

miR-18a mut sense: TCGAGATAGTATGCCCTTAAGACTTAATTTTAACCAAAGGCCTAGCACTACTTTCGGGGCTGCAATAAACACTTAACGCGCGTGCGCACGCGCGCGCGGC

miR-18a mut a/sense: GGCCGCCGCGCGCGCGTGCGCACGCGCGTTAAGTGTTTATTGCAGCCCCGAAAGTAGTGCTAGGCCTTTGGTTAAAATTAAGTCTTAAGGGCATACTATC

miR-19 WT sense: TCGAGCAAAGTTGAATTCTAGGTTTGATTTTTAAGATTTTTTTTTTCTTTTGCACTTTTGAGTCCAATCTCAGTGATGAGGTACCTTCTACTAAATGAGC

miR-19 WT a/sense: GGCCGCTCATTTAGTAGAAGGTACCTCATCACTGAGATTGGACTCAAAAGTGCAAAAGAAAAAAAAAATCTTAAAAATCAAACCTAGAATTCAACTTTGC

miR-19 mut sense: TCGAGCAAAGTTGAATTCTAGGTTTGATTTTTAAGATTTTTTTTTTCTGTTACATTTTTGAGTCCAATCTCAGTGATGAGGTACCTTCTACTAAATGAGC

miR-19 mut a/sense: GGCCGCTCATTTAGTAGAAGGTACCTCATCACTGAGATTGGACTCAAAAATGTAACAGAAAAAAAAAATCTTAAAAATCAAACCTAGAATTCAACTTTGC

Quantitative real-time PCR analysis

Total RNAs were isolated using TRI reagent (Sigma) and treated with a TURBO DNA-free kit (Ambion, Applied Biosystems). For mRNA analysis, cDNAs were prepared using SuperScript III First-Strand Synthesis System for reverse transcription-PCR (Invitrogen). Amplification reactions were

performed using the PowerSYBR Green PCR master mix (Applied Biosystems) with QuantiTect Primer Assays from Qiagen. Target gene expression levels were normalized to actin or glyceraldehyde-3-phosphate dehydrogenase. From the same RNA samples, microRNA expression levels were analyzed starting with 10 ng of total RNA using TaqMan microRNA Assays and the TaqMan Gene expression Master Mix according to the instructions of the manufacturer (Applied Biosystems). Target gene expression levels were normalized to the RNU6B. All quantitative PCR (qPCR) reactions were performed on an ABI 7900 Sequence Detection system and analyzed with RQ Manager software v1.2.

MicroRNA gain-of-function gene expression analysis

HCT116Dicer^{hypo} or DLD1Dicer^{hypo} cells were transfected with 25 nmol/L final concentrations of the indicated microRNA mimics. Total RNA was purified by use of the RNeasy protocol (Qiagen) at the time specified, processed as described previously (20), and hybridized competitively with processed RNA from mock-transfected cells (treated with transfection reagent in the absence of microRNA mimic) to microarrays containing oligonucleotide probes corresponding to ~40,000 human transcripts. Data were analyzed by use of Rosetta Resolver software. Gene regulations were calculated as error-weighted mean $\log_{10}$ ratios from fluor-reversed pairs (two ratio hybridizations were performed with fluorescent label reversal to eliminate dye bias).

Correlating expression levels of MIR17HG and TGFβ-responsive genes

The 318 human cancer cell lines comprising the Wooster data set were classified according to tumor tissue of origin. Relative probe set intensity for each gene of interest and MIR17HG were obtained from the publicly available GlaxoSmithKline microarray database (21) and averaged for cell lines within each tumor type.

Results

Clusterin inhibits tumor growth and angiogenesis

To analyze the functional significance of clusterin downregulation in Myc-mediated tumorigenesis, we transduced RasMyc colonocytes with a retrovirus expressing murine clusterin and/or the puromycin resistance gene and implanted these cells subcutaneously in syngeneic mice. Transduced cells expressed clusterin at higher levels than empty vector–transduced cells but at lower levels than Ras-only colonocytes (Fig. 1A, inset). Despite the modest overexpression achieved, RasMyc tumors with reconstituted clusterin expression grew significantly slower than tumors transduced with the empty vector (Fig. 1A). To determine whether clusterin affects tumor formation by human cells, we used the HCT116 human colon carcinoma cell line which expresses mutant Ki-Ras, elevated levels of Myc and very low levels of clusterin. These cells were also modified to constitutively express the firefly *luciferase* gene, allowing the analysis of tumor growth in live animals using bioluminescent imaging. Thus, modified HCT116 cells were then infected with retroviruses expressing human clusterin or puromycin resistance gene alone. A total of 2×10^6 clusterin-expressing or control cells were implanted subcutaneously on contralateral flanks in nude mice and tumor growth was assessed three times per week. Initially, tumors grew at comparable rates, but eventually, modest clusterin overexpression (Fig. 1B, inset) significantly inhibited the growth of tumor xenografts (Fig. 1B), which was consistent with data from the colonocyte model. Delayed tumor suppression was apparent through the use of optical imaging (Fig. 1C, compare region of interest values at days 3 and 21) and suggested that antiangiogenesis could be involved.

The antiangiogenesis-based mechanism would be consistent with clusterin being a secreted protein (save for some special conditions; ref. 22). This was readily apparent following immunostaining of Ras and RasMyc tumors. Although RasMyc tumor cells were essentially negative for clusterin expression, Ras neoplasms exhibited strong cytoplasmic and extracellular staining (Fig. 1D). As a secreted protein, clusterin could interact with endothelial cells. Additionally, a homology has been noted between amino acids 77 to 98 in clusterin and some TSR repeats (23), which are thought to mediate the antiangiogenic activity of thrombospondin-1 (Fig. 1E). Thus, we set out to explore a possible correlation between clusterin and angiogenesis.

To this end, we used murine colonocytes, which are strongly angiogenic even without transformation by Ras or Myc, perhaps due to the lack of p53 (19). Control and clusterin-overexpressing colonocytes were embedded in Matrigel and injected s.c. into mice, as described previously (6). Seven days later, Matrigel pellets were excised and liquefied, and hemoglobin concentration was measured. We indeed observed >4-fold decrease in hemoglobin content (Fig. 1F), attesting to the intrinsic antiangiogenic properties of clusterin. To determine whether clusterin inhibits tumor angiogenesis, we compared microvascular densities of Clu^{LOW} and Clu^{HIGH} neoplasms. H&E staining clearly showed a marked reduction in large caliber vessels characteristic of RasMyc tumors following clusterin overexpression (Fig. 1G, microphotographs and scatter plot). Because blood vessels in HCT116 xenografts are of smaller caliber, we used staining for the endothelial cell marker CD31. Again, we found that clusterin expression negatively correlated with tumor neovascularization (Fig. 1H, microphotographs and scatter plot). Thus, just like its fellow TSR superfamily member thrombospondin-1, clusterin is an inhibitor of angiogenesis.

miR-17~92 regulates clusterin indirectly through the TGFβ pathway

We then asked whether Myc-mediated repression of clusterin also involves miR-17~92, even though the commonly used TargetScan algorithm (24) does not predict miR-17~92 binding sites within the 3′-UTR of the CLU gene. When the cluster was overexpressed using a CMV promoter–containing retrovirus in Ras-transformed mouse colonocytes, miR-17~92 levels were increased no more than 4-fold and were similar to that observed in RasMyc colonocytes (7; data not shown). Even without gross miR-17~92 overexpression, we observed markedly reduced

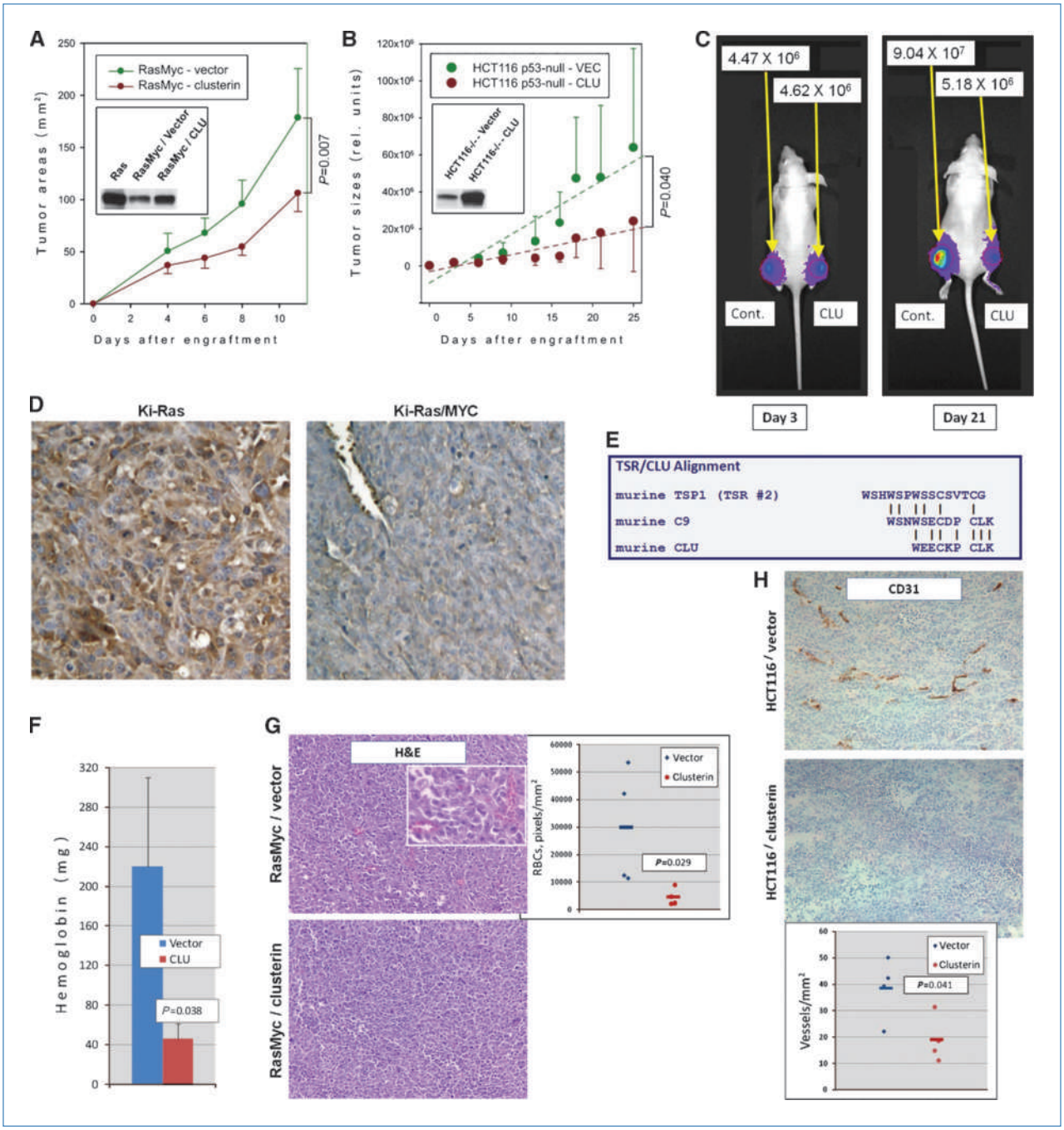

Figure 1. Clusterin inhibits tumor growth and angiogenesis. A, growth of subcutaneous tumors derived from RasMyc cells transduced with a retrovirus expressing murine clusterin and/or the puromycin resistance gene. Inset, immunoblot of clusterin levels in Ras and RasMyc colonocytes. B, growth of subcutaneous tumors derived from HCT116 cells transduced with an empty vector or the retrovirus expressing human clusterin. Regression lines represent average rates of growth. The *P* value refers to the difference in regression coefficients. Inset, immunoblot of clusterin levels in transduced cells. C, *in vivo* bioluminescent imaging of representative animals from the experiment in B. Mice were photographed at days 3 and 21 after injection. No less than five animals per group were used in all these experiments. D, immunohistochemical staining of Ki-Ras and Ki-Ras/Myc tumors with an anti-clusterin antibody. Cytoplasmic staining for clusterin is depicted in brown whereas nuclei are counterstained in blue. E, alignment of the second TSR of murine thrombospondin-1 with the C9 protein and clusterin. F, hemoglobin content of Matrigel pellets 7 d after injection. Matrigels were admixed with p53-null mouse colonocytes transduced with either empty vector (blue bar) or clusterin retrovirus (red bar) and injected s.c. into syngeneic host animals. G, H&E staining of RasMyc/vector (top) and RasMyc/clusterin (bottom) tumor sections. Perfused blood vessels contain numerous RBC, which could be clearly seen under higher magnification (inset). The scatter plot represents densities of perfused blood vessels in four individual tumors. H, immunohistochemical staining of control (top) and clusterin-overexpressing (bottom) HCT116 tumor sections with antibody recognizing the endothelial cell surface antigen CD31. The scatter plot represents the densities of CD31-positive blood vessels in four individual tumors.

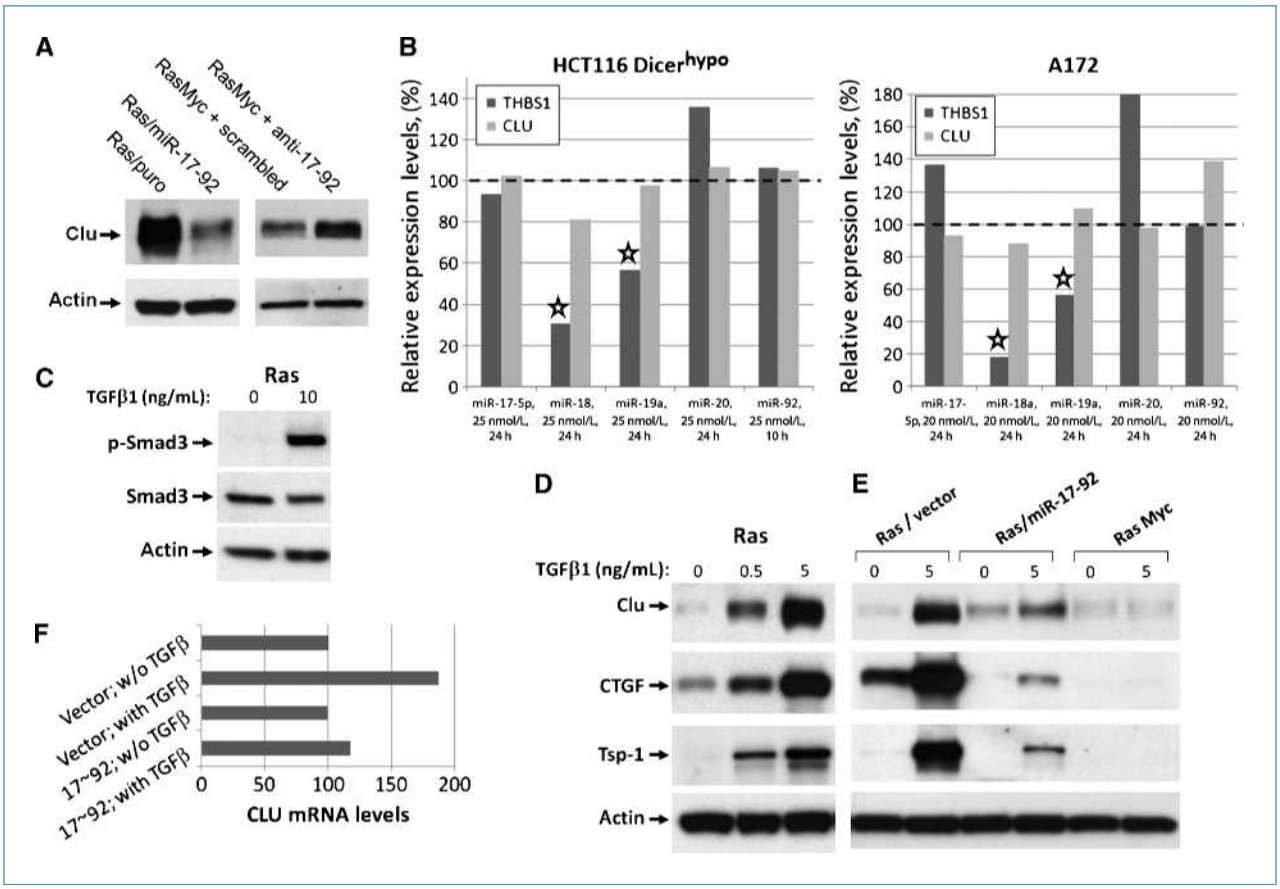

Figure 2. Clusterin is regulated by miR-17~92 via the TGFβ pathway. A, immunoblotting analysis of clusterin expression levels in the following cell lines. Left, Ras-only mouse colonocytes transduced with either empty vector (Ras/Puro) or the miR-17~92–encoding retrovirus (Ras/miR-17~92). Right, RasMyc cells transfected with scrambled or anti–miR-17~92 2′-*O*-methyl oligoribonucleotides. B, changes in expression levels of thrombospondin-1 (THBS1) and clusterin mRNAs in HCT116 Dicer^{hypo} (left) and A172 (right) cells after transfection with the indicated microRNA mimics. mRNA levels in HCT116 and A172 cells were profiled using Affymetrix microarrays and qPCR as described in Materials and Methods. C, activation of TGFβ signaling in Ras colonocytes. Ras cells treated with vehicle or 10 ng/mL of TGFβ1 for 30 min were analyzed by immunoblotting for phosphorylated Smad3 (pSmad3) and total Smad3. D, measurement of TGFβ effects on TSR proteins. Ras cells were treated with increasing doses of TGFβ1 for 48 h and lysates were immunoblotted for clusterin and CTGF proteins. Tsp-1 was detected in conditioned medium. E, immunoblotting analysis of TSR proteins in Ras/vector, Ras/miR-17~92 or c-Myc cells cultured in the absence or presence of TGFβ1 (5 ng/mL) for 48 h. F, CLU mRNA levels in Ras/vector and Ras/17~92 cells before and after (24 h) stimulation with TGFβ, as measured by qPCR. Expression levels of CLU are adjusted to those of glyceraldehyde-3-phosphate dehydrogenase.

levels of clusterin by immunoblotting (Fig. 2A, left). Conversely, the knockdown of all six members of the miR-17~92 cluster with 2′-*O*-methyl antisense oligoribonucleotides partially restored clusterin expression in RasMyc colonocytes (Fig. 2A, right).

We then analyzed the immediate effects of these microRNAs on clusterin mRNA levels in HCT116 cells rendered hypomorphic for Dicer through the deletion of its helicase domain in exon 5 (17). This mutation causes HCT116 Dicer^{hypo} cells to express low levels of endogenous microRNAs, making them well-suited for gain-of-function experiments (25, 26). They were transfected with microRNA mimics and gene expression was profiled at short intervals (10–24 h) to capture only those mRNAs that were directly affected by introduced miRs. Under these conditions, thrombospondin-1 mRNA was appreciably downregulated by miR-18a and 19a, as envisioned in our previous study (7); however, none of the six miR-17~92 members were found to lower clusterin mRNA levels significantly (Fig. 2B, left). Identical data were obtained using another colon cancer cell line with the Dicer mutation (DLD1 Dicer^{hypo}; data not shown). To determine if clusterin mRNA "resistance" to miR-17~92 mimics was an artifact of the Dicer mutation, we performed the same experiment in Dicer-sufficient A172 cells where miR mimics were found to work effectively,[5] with essentially identical results (Fig. 2B, right). Furthermore, no effects of miR-17~92 mimics on clusterin protein expression were detected (data not shown). Taken together, these data suggest that clusterin is not a direct target for miR-17~92 and that instead miR-17~92 targets an upstream activator of clusterin expression. Reports from one laboratory showed that in some cell lines, clusterin

[5] J.L. Fox and A. Thomas-Tikhonenko, unpublished data.

could be induced by TGFβ (27), prompting us to investigate this pathway as a possible link between miR-17~92 and CLU.

To confirm that parental Ras colonocytes (unlike most human colon carcinomas) are responsive to TGFβ, we stimulated them with recombinant human TGFβ1 for 30 minutes and observed robust phosphorylation of Smad3 (Fig. 2C). We then examined the expression of clusterin and several other TSR proteins in TGFβ-treated Ras cells. Clusterin was indeed induced in a dose-dependent manner by TGFβ, as were CTGF and thrombospondin-1 (Fig. 2D).

Remarkably, when we examined clusterin protein levels after TGFβ treatment in Ras cells overexpressing either miR-17~92 or c-Myc, we discovered that upregulation of clusterin was either nonexistent (in the presence of Myc) or strongly inhibited (in the presence of retrovirally encoded miR-17~92). The same pattern of expression was observed for thrombospondin-1 and CTGF (Fig. 2E). Additionally, CLU mRNA induction by TGFβ was apparent in control but abolished in miR-17~92–transduced cells (Fig. 2F). This suggests that Myc might inhibit the expression of TSR proteins either directly or indirectly by interfering with the TGFβ signaling pathway, at least in part through the induction of miR-17~92. Although thrombospondin-1 and CTGF could be targeted both directly and indirectly, the prime example of the TGFβ-dependent deregulation is the Myc-clusterin axis.

miR-17~92 downregulates endogenous TGFβ receptor II and Smad4

The TGFβ pathway is activated when the cognate ligand binds to the type II receptor (TGFBR2) at the cell surface and recruits and phosphorylates the type I receptor (TGFBR1). This heterodimeric transmembrane complex further phosphorylates Smad2 and Smad3, allowing them to form a complex with Smad4. The Smad2/3-Smad4 complex then translocates to the nucleus where it can either promote or inhibit transcription of target genes (28, 29). We wanted to determine which of these proteins are affected by miR-17~92.

Previously, miR-17 and miR-20a (with identical seed sequences) were shown to inhibit expression of the luciferase reporter when it was fused to the 3′-UTR of TGFBR2 (30). However, this repression had not been observed in the context of the endogenously expressed receptor, which became the focus of the next series of experiments.

To reconfirm that TGFBR2 is a direct target of miR-17/20a, we generated two psiCHECK-2–based bicistronic firefly/renilla luciferase sensor vectors, wherein the coding sequence of the Renilla luciferase is followed by ~100 nucleotide synthetic DNA fragments encompassing the predicted miR-17/20a binding site from TGFBR2 3′-UTR in either wild-type or seed-mutated conformation (see Materials and Methods). The recombinant constructs were transfected into DLD1 Dicer^{hypo} cells along with miR-17 or control mimic. Consistent with *in silico* predictions and published data (30), inclusion of the miR-17/20a site decreased protein output in a manner dependent on cotransfection with the cognate miR and retention of the intact seed homology sequence (Fig. 3A). This suggests that TGFBR2 is indeed a direct target of miR-17/20a.

To extend our observation to the endogenous transcript, we then transfected the corresponding mimics into DLD1 Dicer^{hypo} cells. Once again, transfection of miR-17 and miR-20a but not other members of the cluster into these cells resulted in reduced TGFBR2 mRNA levels (Fig. 3B, asterisks). However, TGFBR2 protein levels could not be studied in common human colon cancer cell lines such as HCT116 or DLD1 because they are microsatellite-instable and have mutations crippling TGFBR2 expression (31). We thus performed this analysis in Ras colonocytes.

To verify that TGFBR2 levels control clusterin expression in these cells, we transfected Ras cells with a pool of siRNAs against TGFBR2 and observed a concomitant decrease in TGFBR2 and clusterin (Fig. 3C). To test whether miR-17~92 targets endogenous TGFBR2, we transfected each miR-17~92 mimic into Ras colonocytes. We found that miR-17 and miR-20a reduced TGFBR2 protein levels 20 hours after transfection most strongly, whereas miR-18a mimic had a modest effect (Fig. 3D, top). To assure accurate measurements, bands were quantified using a LI-COR Biosciences Odyssey Infrared Imager and appropriate IRDye-labeled antibodies (Fig. 3D, bottom). To determine if reduced TGFBR2 levels affect Smad3 activation, we treated cells transfected with miR-17, miR-18a, and miR-20a with TGFβ and measured levels of total and phosphorylated Smad3. Again, although steady-state levels of Smad3 remained constant, pSmad3 levels were reduced in miR-17 and miR-20a–transfected cells, as measured by imaging of Western blots (Fig. 3E, top and bottom).

To determine whether other mediators of TGFβ signaling could also be among the miR-17~92 targets, we evaluated levels of the receptor-regulated Smads (Smad2 and Smad3) and the principal co-Smad (Smad4) in the presence of overexpressed miR-17~92. Immunoblotting revealed that Smad2 and Smad3 levels were unaffected by miR-17~92, but Smad4 levels were appreciably lower in miR-17~92–transduced cells (Fig. 4A). To determine if this regulation also occurs in human colon cancer cell lines, we transfected DLD1 Dicer^{hypo} cells with a mixture of all six 17~92 mimics and measured Smad4 protein levels 24 and 48 hours after transfection. At both time points, Smad4 levels were more than 2-fold lower than in control mimic-transfected cells (Fig. 4B).

We wanted to determine how miR-17~92 regulates Smad4 expression because Smad4, a tumor suppressor gene predominantly involved in gastrointestinal tumorigenesis, has been reported to affect angiogenesis (32) but has not been proven to be a target of any specific microRNA. To this end, we transfected DLD1 Dicer^{hypo} cells with individual mimics and measured Smad4 mRNA levels. Interestingly, all miR-17~92 mimics tested decreased Smad4 mRNA levels, but this downregulation was most profound with miR-18a (Fig. 4C). In the human Smad4 3′-UTR, TargetScan predicts binding sites for miR-17 and miR-19 as well as miR-18a. To determine whether any of these were bona fide target sites, we constructed six sets of psiCHECK2-based

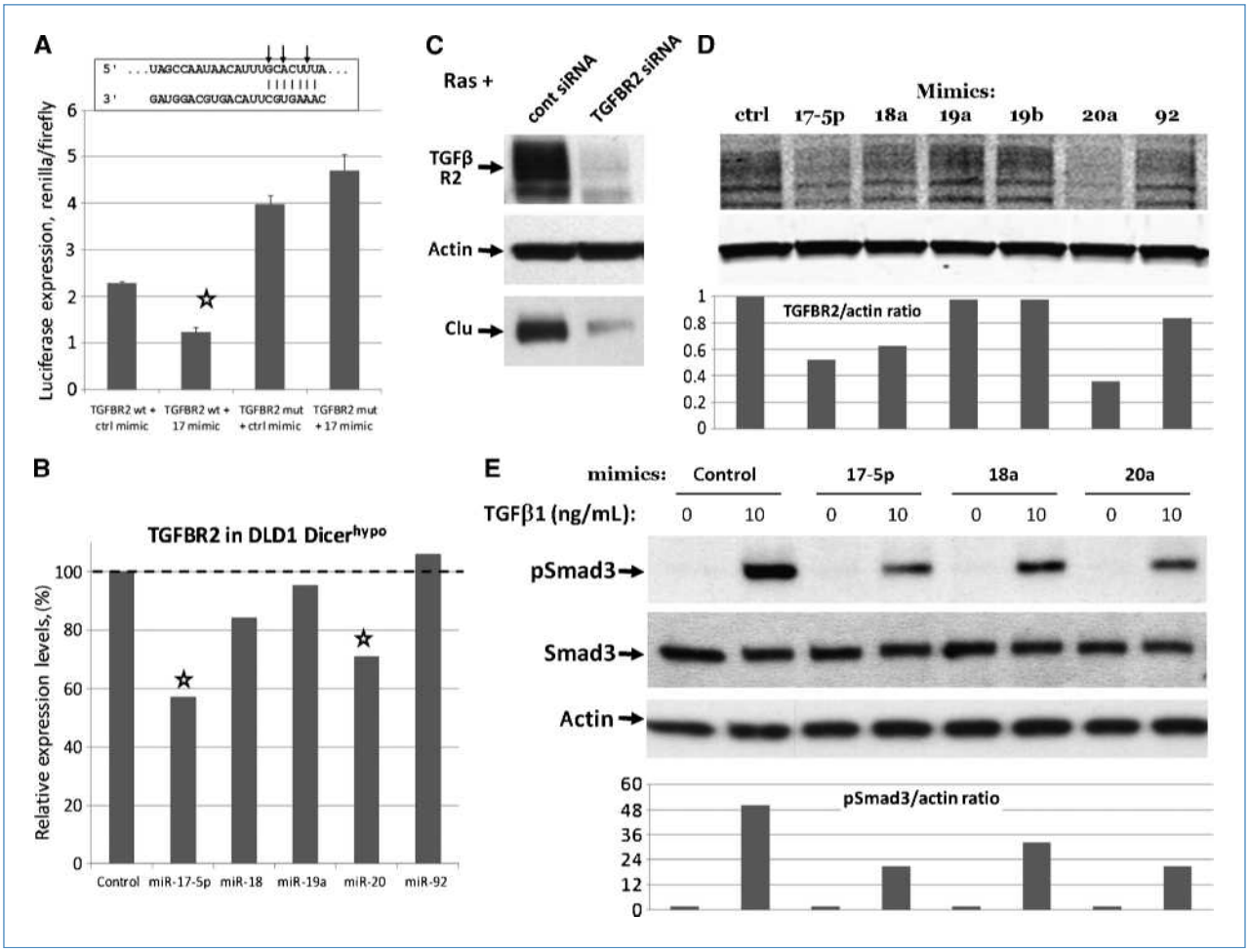

Figure 3. miR-17~92 targets endogenous TGFβ receptor II. A, luciferase sensor assay. Constructs tested were psiCHECK-2 derivatives containing a single miR-17/20a binding site from TGFBR2 3′-UTR in either wild-type (wt) or seed-mutated (mut) conformation. Cells were additionally cotransfected with miR-17 or control mimic. Results are expressed as ratios of renilla to firefly luciferase, the latter being constitutively expressed from the same vector and serving as a control for transfection efficiency. Sequence alignment corresponds to positions 268 to 274 of TGFBR2 3′-UTR and mature hsa-miR-17. Arrows indicate mutated nucleotides. B, expression levels of TGFBR2 mRNA in DLD1 Dicer^{hypo} cells 10 h after transfection with microRNA mimics (25 nmol/L). mRNA levels were quantified by microarray. C, immunoblotting analysis of TGFBR2 and clusterin expression levels in Ras cells transfected with 10 nmol/L of nontargeting siRNA pool or siRNA pool targeting mouse TGFBR2. D and E, immunoblotting analysis of TGFBR2 and Smad3 in Ras cells 20 h after transfection with microRNA mimics (25 nmol/L). Bottom, quantitations of Western blots above.

sensor plasmids as described above. DLD1 Dicer^{hypo} cells were transfected with these constructs and also control or cognate mimics. The results in Fig. 4D show that of the three sequences tested, only the miR-18a homology region is a bona fide binding site. Not only did transfection with miR-18a mimic reduce protein output (asterisk in column 2), but it was restored (albeit partly) when the seed homology sequence was mutated (double asterisk in column 4). That the mutant construct was still partially sensitive to the miR-18a mimic could be attributed to the fact that the mir-18a site in Smad4 contains additional base pairing at the 3′ end, which might increase the tolerance of mutations in the seed sequence (33). Of note, this set of mutations was designed to be subtle and resulted in a single one-nucleotide bulge (Fig. 4D, right, middle arrow). Still, the importance of this site is underscored by its conservation among primates, macaques, mouse, rat, and guinea pig (24). Additionally, other microRNAs in the miR-17~92 cluster, which fail to target the reporter constructs tested but do affect the endogenous mRNA levels, might be affecting Smad4 indirectly or through alternative binding sites.

miR-17~92 host transcript levels inversely correlate with those of many TGFβ target genes

Concurrent downregulation of both TGFBR2 and Smad4 by miR-17~92 cluster components suggested that this cluster could be a global attenuator of TGFβ signaling in various cell types. To corroborate this hypothesis, we took advantage of existing profiling studies, primarily of the Wooster data set generated by GlaxoSmithKline and made available through the National Cancer Institute caArray portal (21). This data set contains gene expression profiling data from 318 tumor

cell lines. Notably, it documents the expression levels of MIR17HG, the miR-17~92 primary transcript (Affy_ID 232291_at). To simplify analysis, the cell lines were grouped in 32 tumor types based on tissue of origin, and regression analysis was carried out to identify genes whose expression levels inversely correlate with that of MIR17HG. Provocatively, genes ranking no. 1 and no. 2, respectively, were *thbs1* (encoding thrombospondin-1) and CTGF, two known miR-17~92 targets (7) for which r^2 exceeded 0.75 (Fig. 5B). That known targets of miR-17~92 topped the list was construed as a validation of this bioinformatics approach.

We thus asked whether known TGFβ targets that are not targeted by miR-17~92 directly would also show inverse correlation with miR-17~92. To this end, we considered all genes upregulated by TGFβ at least 2-fold in all four different cell lines profiled in a recent study (34). The 12 genes that fit these criteria were as follows: *ANGPTL4, BHLHB2/BHLHE40, CTGF, IL11, JUN, NEDD9, LARP6, RHOB, SERPINE1, SKIL, SMAD7*, and *ZEB1*. We assessed their expression levels in both HCT119 and DLD1 Dicer^{hypo} cells transfected with individual mimics and excluded all genes showing downregulation by at least one mimic in at least one cell line, an indicator of potential TGFβ-independent regulation (cyan squares in the heatmap in Fig. 5A). Additionally, we excluded SMAD7 and RHOB as they had predicted conserved miR-17~92 binding sites per TargetScan. This left us with five genes (*ANGPTL4, IL11, JUN, LARP6*, and *ZEB1*) that could be reasonably considered to be miR-17~92 nontargets, and we added *CLU* to that list based on the data shown in Fig. 2B. Regression analysis revealed that five out of six genes analyzed (with the exception of ZEB1) negatively correlated with MIR17HG, with r^2 ranging from 0.38 to 0.69 (Fig. 5B). Interestingly, four out of eight genes (*THBS1, CTGF, CLU*, and *ANGPTL4*; dotted red rectangle) are known to encode proteins with antiangiogenic properties (for Angptl4 data, see ref. 35). This led us to propose a mechanism whereby multiple inhibitors of angiogenesis are downregulated by miR-17~92, either directly or via suppression of TGFβ signaling (Fig. 5C).

Modest overexpression of miR-17~92 impairs gene regulation by TGFβ

The inverse correlation between MIR17HG levels and those of TGFβ target genes implied that most of the cell lines

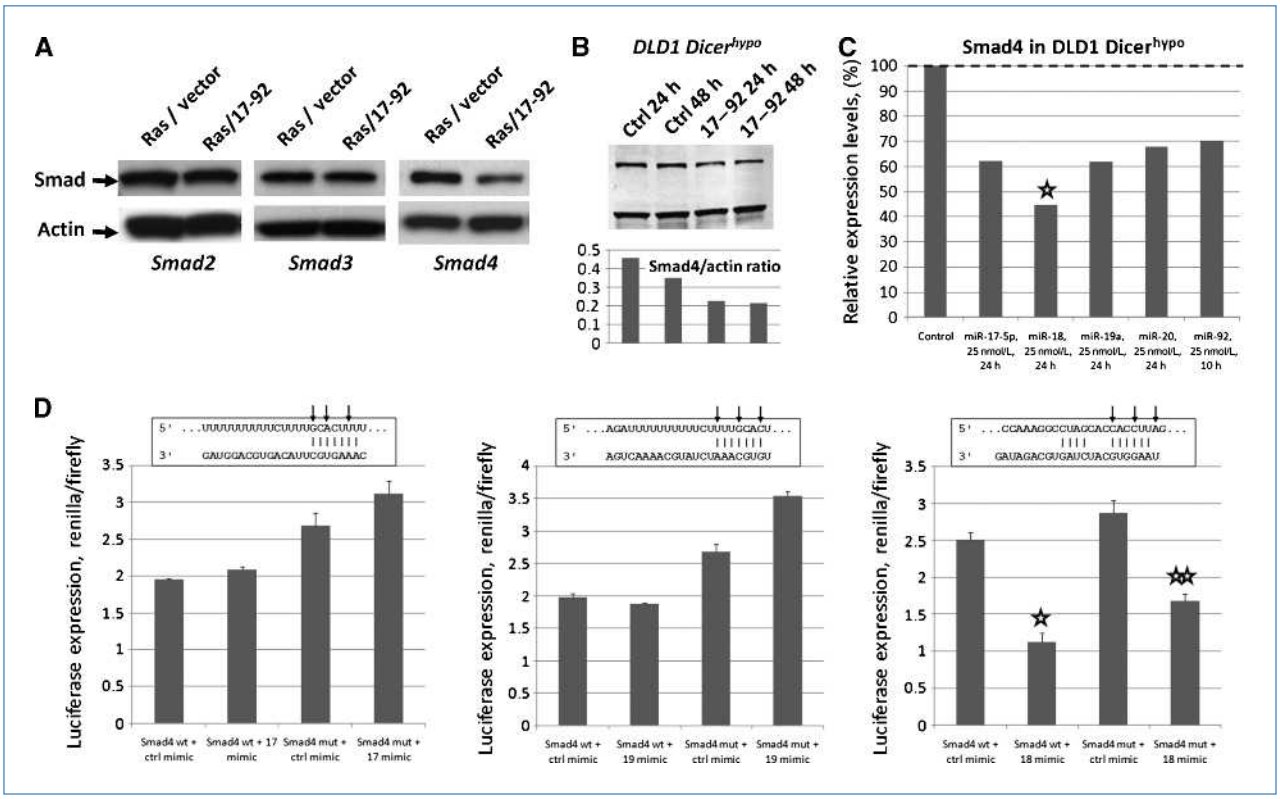

Figure 4. miR-17~92 inhibits expression of Smad4. A, immunoblotting for Smad2, Smad3, and Smad4 in stably transduced Ras/vector and Ras/miR-17~92 cells. B, immunoblotting for Smad4 in DLD1 Dicer^{hypo} cells 24 and 48 h after transfection with control mimic or the mix of six 17~92 mimics. The ratio of Smad4-to-actin is plotted below. C, Smad4 mRNA expression levels in DLD1 Dicer^{hypo} cells 24 h after transfection with five individual 17~92 mimics (miR-19b was not tested), as analyzed by microarray. Asterisk indicates the most profound downregulation of Smad4 mRNA, although in all five transfections, statistically significant downregulation was observed. D, luciferase reporter assay performed on predicted miR-17, miR-19, and miR-18a binding sites in the human Smad4 gene. Results are expressed as a ratio of renilla to firefly luciferase. Sequence alignment corresponds with positions 1357 to 1363, 1354 to 1360, and 5491 to 5497 of Smad4 3′-UTR and mature hsa-miR-17, -19a, and -18a, respectively. Arrows indicate mutated nucleotides.

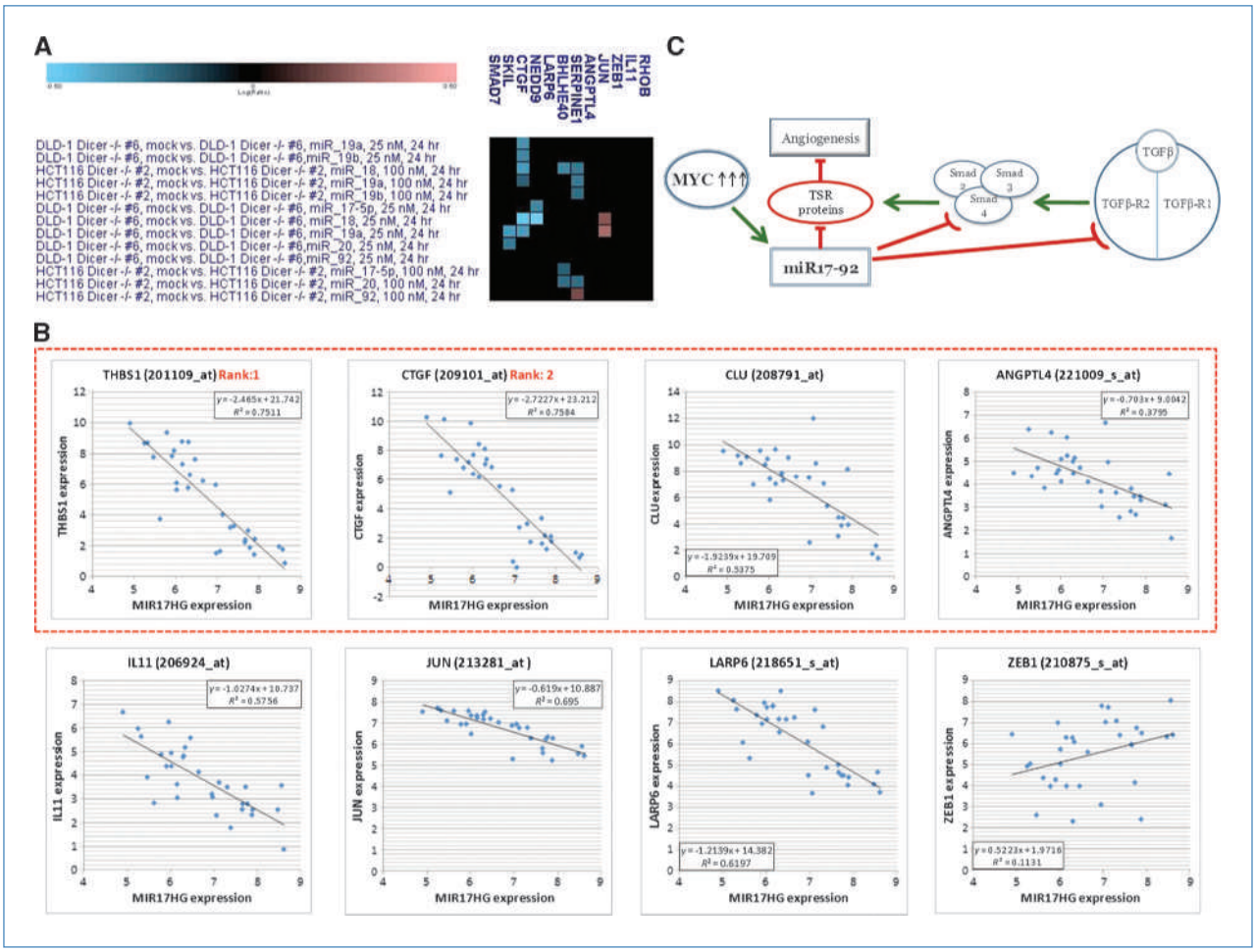

Figure 5. Inverse correlation between MIR17HG levels and those of TGFβ target genes. A, expression levels of TGFβ target genes in Dicer-deficient cell lines transfected with individual 17~92 mimics. In the heatmap, cyan and magenta squares denote downregulated and upregulated genes, respectively. B, regression analysis performed on individual TGFβ target genes and MIR17HG. Each dot represents an individual tumor type. The dotted red rectangle denotes genes encoding known regulators of angiogenesis. C, the proposed connections between Myc–miR-17~92 axis, TGFβ pathway, TSR proteins, and angiogenesis.

profiled produce and respond to endogenous TGFβ in an autocrine fashion. Another implicit assumption was that levels of MIR17HG correlate with those of mature 17~92 microRNAs. To test the effect of miR-17~92 on TGFβ signaling in a more defined setting, we wanted to identify cell lines with low miR-17~92 expression levels, transduce them with a miR-17~92 retrovirus, verify downregulation of TGFβ signaling components, and assess responses to exogenous TGFβ.

To this end, we first analyzed MIR17HG levels across tumor types. Using the same Wooster data set, we observed that glioblastomas and hepatocellular carcinomas have low MIR17HG levels (Fig. 6A, black rectangles) We then chose four cell lines, three glioblastomas (A172, SF268, and U251), and one hepatocellular carcinoma (HepG2), and transduced them with the same miR-17~92 retrovirus as used previously for Ras colonocytes (7). To assess the overexpression level, we measured the levels of miR-18a and miR-20a using qPCR. As expected, they were modestly elevated (2- to 8-fold) in transduced cells (Fig. 6B). Furthermore, in these cells, the levels of TGFBR2 and Smad4 were appreciably lower than in "empty vector" cultures, whereas the levels of Smad2 and Smad3 were unchanged (Fig. 6C), consistent with data in Figs. 3 and 4.

We then measured the expression levels of five TGFβ "signature" genes: *ANGPTL4, CLU, IL11, JUN*, and *LARP6*. *CLU* was not induced by TGFβ in any of these cell lines and we were unable to detect *IL11* mRNA (data not shown). For the remaining three genes, we observed consistent upregulation by TGFβ in vector-transduced cells (Fig. 6D). However, when vector- and miR-17~92–transduced cells were compared side by side, in all cases except one (*ANGPTL4* in SF268 cells), activation by TGFβ was less robust in miR-17~92–transduced cells (Fig. 6E). We thus concluded that attenuation by miR-17~92 of TGFβ signaling is not limited to TSR proteins and affects many other genes, presumably those for which TGFRB2 and Smad4 levels are rate-limiting.

To determine which microRNA(s) in the miR-17~92 cluster are primarily responsible for the observed effects, we transfected A172 cells with individual mimics as well as with admixed microRNAs and determined their effects on gene activation by TGFβ using ANGPTL4 as an example. As evidenced by data in Fig. 6F, of all members of the cluster, miR-18a exerted the most profound negative effects (asterisk) comparable in scope to that caused by the admixed mimics. This result identifies this microRNA as a key attenuator of TGFβ signaling, at least in this particular cell type.

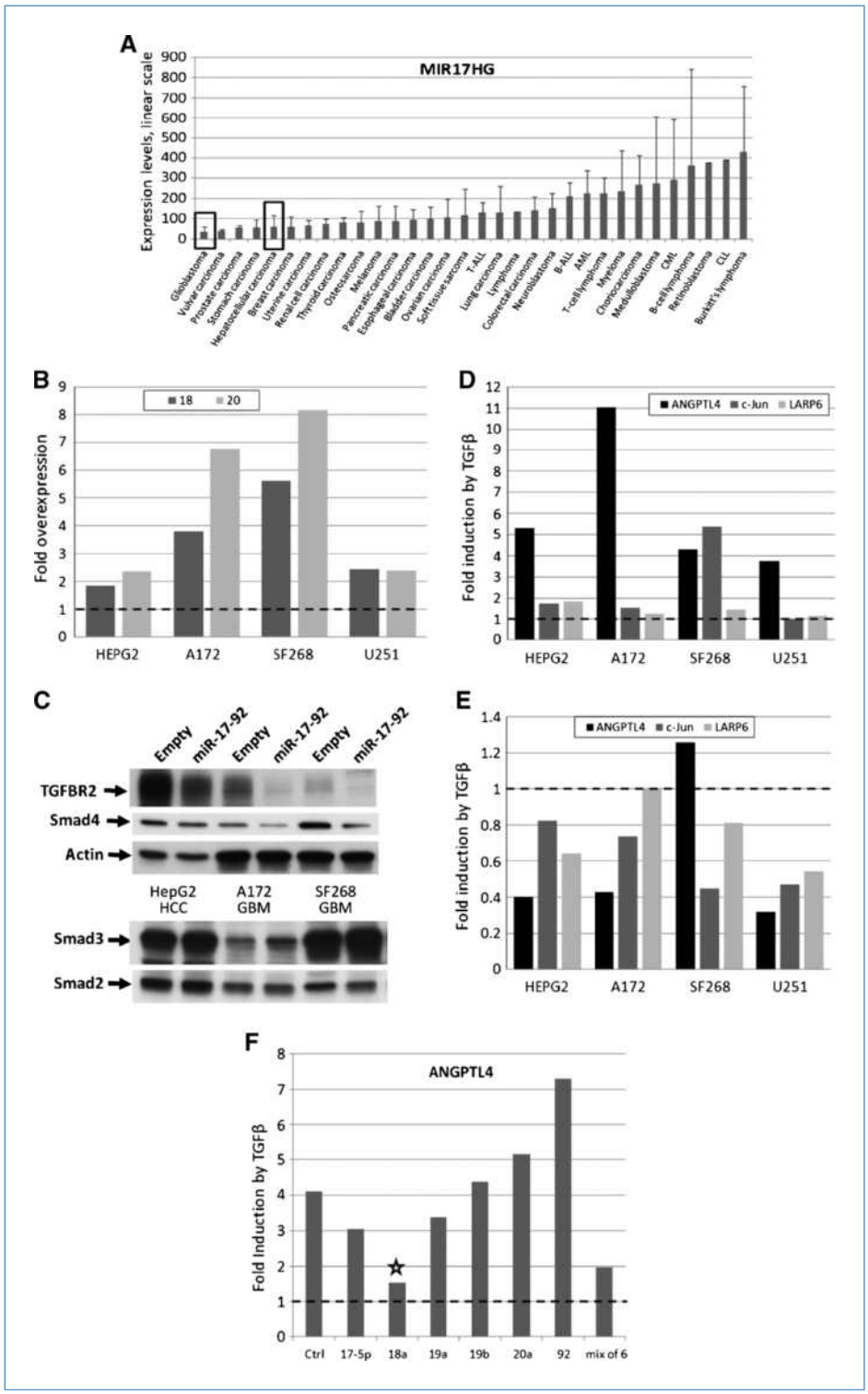

Figure 6. miR-17~92 impairs gene regulation by TGFβ. A, expression levels of MIR17HG across tumor types from the Wooster data set. Bars, SD. T-ALL, acute T-cell lymphoblastic leukemia; B-ALL, acute B-cell lymphoblastic leukemia; AML, acute myeloid leukemia; CML, chronic myeloid leukemia; CLL, chronic lymphoblastic leukemia. B, fold overexpression of miR-18 and miR-20 in miR-17~92–tranduced glioblastoma (GBM) and hepatocellular carcinoma (HCC) cell lines relative to empty vector–transduced cells, as measured by qPCR. C, expression levels of TGFBR2 and Smad proteins in cell lines depicted in the previous panel, as measured by Western blotting. D, fold induction by TGFβ of three transcripts in the same cell lines as measured by qPCR. Treatment with TGFβ was carried out as in Fig. 2. E, comparison by qPCR of TGFβ effects on gene expression in miR-17~92–transduced cells relative to empty vector–transduced cells. F, comparison by qPCR of TGFβ effects on ANGPTL4 in control (Ctrl) and miR-17~92 mimic–transfected A172 cells.

Discussion

TGFβ and Myc have long been linked in the context of cell cycle progression, where the former is to the latter as yin is to yang. Indeed, TGFβ-induced growth arrest inevitably involves downregulation of c-Myc and conversely, during Myc-induced transformation, cells become refractory to the inhibitory effects of TGFβ (36). This interdependent, antagonistic relationship is commonly explained by a model in which Myc (along with its interactor Miz1) and Smad2/3/4 compete for the binding to promoters of cyclin-dependent kinase inhibitors, such as p21Cip1, p15Ink4b, and possibly p27Kip1 (37). In proliferating cells, these promoters are occupied by the Myc/Miz1 complex resulting in CDKI gene repression and cell cycle progression (38, 39). Upon exposure to TGFβ, Smad complexes gain the upper hand, induce CDKI expression, and block entry into the cell cycle (reviewed in refs. 29, 40).

Assuming that Myc must blunt the TGFβ responses to establish the transformed phenotype, this approach to TGFβ inhibition is surprisingly ineffective because every target gene would need to be dealt with individually. The better way would be to intercept the TGFβ signal before it reaches the nucleus. Yet there was surprisingly little evidence that Myc employs this strategy. There is one published report showing that Myc binds to Smad2 and Smad3, but rather than inhibiting their transcriptional activity, Myc inhibits the Smad-dependent activity of Sp1. Thus, such effects are presumably limited to promoters containing both Smad2/3 and Sp1 binding sites (41). Although TGFBR2 has been reported to be downregulated by c-Myc in B-cells, there was no evidence of direct promoter binding, and consequently, the mechanism of downregulation remained unknown (42). Furthermore, the Myc Target Gene database does not include any of the Smads (43). However, the discovery of Myc-regulated microRNAs (10, 12) highlighted the possibility that some components of the TGFβ pathway could be affected by Myc indirectly through microRNA clusters such as miR-17∼92.

The effects of microRNAs, including miR-17∼92, on TGFβ target genes are well-recognized. For example, in 2008, two articles detailed how miR-200 and miR-205 directly target TGFβ-responsive genes ZEB1 and ZEB2, thus contributing to epithelial-mesenchymal transition (44, 45). More relevantly, miR-17∼92 also targets important TGFβ target genes, such as p21 (46) and most notably Bim (46–51). Yet these important articles offered no evidence of the systemic effects of microRNA on the TGFβ pathway. In fact, the reverse seems to be true: Smad proteins are known to control Drosha-mediated microRNA maturation (52). Thus, prior studies reinforced the prevailing view that miR-17∼92 impairs TGFβ signaling by inhibiting the transcription of individual TGFβ-responsive genes (53). This model was agnostic of possible targeting of TGFβ receptors and Smads; yet it was attractive because it incorporated miR-17∼92 into the Myc-TGFβ axis and provided a mechanistic explanation for miR-17∼92 overexpression (i.e., via Myc activation).

On the other hand, a couple of very recent articles showed targeting by other miRs of various Smads. Relevant examples include the report of targeting of SMAD5 by miR-155 in diffuse large B-cell lymphoma (54). Although this event might have implications for B-lymphomagenesis, what accounts for overexpression of miR-155 remains an open question. Similarly, another study showed that miR-23b inhibits multiple Smads and promotes hepatocyte differentiation at the expense of cholangiocyte fate determination and bile duct formation (55). Yet how the miR-23b cluster is turned on was unclear. Overall, without knowing what controls the miR-based TGFβ switch, the understanding of the decision-making process remained incomplete.

In this study, we show that miR-17∼92 blunts TGFβ responses in colon cancer cells by directly targeting its receptor and the key effector Smad4. Moreover, these events are firmly placed downstream of Myc, which is a direct transcriptional regulator of miR-17∼92 (7, 12). Although TGFBR2 and SMAD4 are known to be genetically inactivated in a subset of colon cancers with microsatellite instability, our data provide evidence that they could be repressed by Myc-regulated microRNAs in non–microsatellite-instable tumors, which frequently overexpress c-Myc and exhibit DNA copy number gain of the miR-17∼92 locus on 13q31 (56). Myc and miR-17∼92 are known to cooperate in other tumor types as well, in particular, in lymphoid tissues (57–59). Finally, our findings are likely to apply to *N*-Myc, which is known to upregulate miR-17∼92 in neuroblastomas and medulloblastomas (14, 60–62).

This provides a mechanistic explanation for two much broader biological questions: how does Myc counteract the tumor-suppressive effects of TGFβ, and how does it promote tumor angiogenesis? Our new data show that by increasing miR-17∼92 levels and blunting TGFβ signaling, Myc could downregulate a wider repertoire of antiangiogenic factors than we appreciated previously. Notably, the revised list now includes clusterin (a.k.a. apolipoprotein J). Although a direct effect of clusterin on tumor angiogenesis has not been previously reported, it was identified as a gene silenced in tumor-conditioned endothelial cells (63). Clusterin downregulation stimulated the growth and sprouting of endothelial cells and the repression of clusterin increased endothelial cell migration. Indeed, the ability of clusterin to inhibit angiogenesis might not be surprising given the homology between clusterin and some TSR proteins (23). Overall, putting the antiangiogenic activity of clusterin, thrombospondin-1, and other TSR proteins in the context of colon carcinoma progression highlights the importance of cell-extrinsic mechanisms in cancer.

Disclosure of Potential Conflicts of Interest

M.A. Cleary is an employee of Merck & Co. Inc. The other authors disclosed no potential conflicts of interest.

Acknowledgments

We are indebted to Drs. Anil Rustgi and Cameron Johnstone (University of Pennsylvania), Lars French (University of Zurich), Sabina Pucci (University of Rome "Tor Vergata"), and Arturo Sala (University College London) for sharing unpublished data on clusterin and Monica Lee (University of Pennsylvania) for the analysis of clusterin-overexpressing clones. We thank Dr. Andrei Bakin (Roswell Park Cancer Institute) for pointing out the overlap between Myc- and TGFβ-regulated genes. Past and current members of our laboratories (in particular Drs. Cinzia Sevignani and Elena Sotillo Piñeiro) are acknowledged for many stimulating discussions, and Dr. Tom Curran (Children's Hospital of

Philadelphia) for general guidance. Dr. Jim Zhe Zhang from the Children's Hospital of Philadelphia Bioinformatics Core contributed to the analysis of the Wooster data set. We are grateful to the Rosetta Gene Expression Laboratory for performing microarray hybridization experiments and Miho Kibukawa (Merck & Co., Inc.) for technical support.

Grant Support

NCI grant R01 CA122334, pilot funds from the NCI grant P30 CA016520, and NIDDK grant P30 DK050306, the Institutional Development Fund of the Children's Hospital of Philadelphia (A. Thomas-Tikhonenko), Cancer Research Institute Immunobiology training grant (J.L. Fox), and NCI training grant T32 CA009140 (P. Sundaram). Optical Imaging Core of the Small Animal Imaging Facility at the University of Pennsylvania was supported in part by NCI grant U54 CA105008.

The costs of publication of this article were defrayed in part by the payment of page charges. This article must therefore be hereby marked *advertisement* in accordance with 18 U.S.C. Section 1734 solely to indicate this fact.

Received 07/07/2010; accepted 07/19/2010; published OnlineFirst 10/12/2010.

References

1. Meyer N, Penn LZ. Reflecting on 25 years with MYC. Nat Rev Cancer 2008;8:976–90.
2. Shchors K, Evan G. Tumor angiogenesis: cause or consequence of cancer? Cancer Res 2007;67:7059–61.
3. Pelengaris S, Littlewood T, Khan M, Elia G, Evan GI. Reversible activation of c-Myc in skin: induction of a complex neoplastic phenotype by a single oncogenic lesion. Mol Cell 1999;3:565–77.
4. Shchors K, Shchors E, Rostker F, Lawlor ER, Brown-Swigart L, Evan GI. The Myc-dependent angiogenic switch in tumors is mediated by interleukin 1β. Genes Dev 2006;20:2527–38.
5. Brandvold KA, Neiman P, Ruddell A. Angiogenesis is an early event in the generation of myc-induced lymphomas. Oncogene 2000;19:2780–5.
6. Ngo C, Gee MS, Akhtar N, et al. An *in vivo* function for the transforming myc protein: elicitation of the angiogenic phenotype. Cell Growth Differ 2000;11:201–10.
7. Dews M, Homayouni A, Yu D, et al. Augmentation of tumor angiogenesis by a Myc-activated microRNA cluster. Nat Genet 2006;38:1060–5.
8. Janz A, Sevignani C, Kenyon K, Ngo C, Thomas-Tikhonenko A. Activation of the Myc oncoprotein leads to increased turnover of thrombospondin-1 mRNA. Nucleic Acids Res 2000;28:2268–75.
9. Ghildiyal M, Zamore PD. Small silencing RNAs: an expanding universe. Nat Rev Genet 2009;10:94–108.
10. Chang T-C, Yu D, Lee Y-S, et al. Widespread microRNA repression by c-Myc promotes tumorigenesis. Nat Genet 2008;40:43–50.
11. Lin CH, Jackson AL, Guo J, Linsley PS, Eisenman RN. Myc-regulated microRNAs attenuate embryonic stem cell differentiation. EMBO J 2009;28:3157–70.
12. O'Donnell KA, Wentzel EA, Zeller KI, Dang CV, Mendell JT. c-Myc-regulated microRNAs modulate E2F1 expression. Nature 2005;435:839–43.
13. Thomas-Tikhonenko A, Viard-Leveugle I, Dews M, et al. Myc-transformed epithelial cells down-regulate clusterin which inhibits their growth *in vitro* and carcinogenesis *in vivo*. Cancer Res 2004;64:3126–36.
14. Chayka O, Corvetta D, Dews M, et al. Clusterin, a haploinsufficient tumour suppressor gene in neuroblastomas. J Natl Cancer Inst 2009;101:663–77.
15. Trougakos IP, Djeu JY, Gonos ES, Boothman DA. Advances and challenges in basic and translational research on clusterin. Cancer Res 2009;69:403–6.
16. Sevignani C, Wlodarski P, Kirillova J, et al. Tumorigenic conversion of p53-deficient colon epithelial cells by an activated Ki-ras gene. J Clin Invest 1998;101:1572–80.
17. Cummins JM, He Y, Leary RJ, et al. The colorectal microRNAome. Proc Natl Acad Sci U S A 2006;103:3687–92.
18. Suh E, Zhengqi W, Swain GP, Tenniswood M, Traber PG. Clusterin gene transcription is activated by caudal-related homeobox genes in intestinal epithelium. Am J Physiol 2001;280:G149–56.
19. Hunter CA, Yu D, Gee M, et al. Cutting edge: systemic inhibition of angiogenesis underlies resistance to tumors during acute toxoplasmosis. J Immunol 2001;166:5878–81.
20. Hughes TR, Mao M, Jones AR, et al. Expression profiling using microarrays fabricated by an ink-jet oligonucleotide synthesizer. Nat Biotechnol 2001;19:342–7.
21. Wooster R. Transcript profiling of cancer cell line panel. Available from: https://array.nci.nih.gov/caarray/project/woost-00041 2008.
22. Yang CR, Leskov K, Hosley-Eberlein K, et al. Nuclear clusterin/XIP8, an X-ray-induced Ku70-binding protein that signals cell death. Proc Natl Acad Sci U S A 2000;97:5907–12.
23. Jenne DE, Tschopp J. Clusterin: the intriguing guises of a widely expressed glycoprotein. Trends Biochem Sci 1992;17:154–9.
24. Grimson A, Farh KK, Johnston WK, Garrett-Engele P, Lim LP, Bartel DP. MicroRNA targeting specificity in mammals: determinants beyond seed pairing. Mol Cell 2007;27:91–105.
25. Linsley PS, Schelter J, Burchard J, et al. Transcripts targeted by the microRNA-16 family cooperatively regulate cell cycle progression. Mol Cell Biol 2007;27:2240–52.
26. Chung EY, Dews M, Cozma D, et al. c-Myb oncoprotein is an essential target of the dleu2 tumor suppressor microRNA cluster. Cancer Biol Ther 2008;7:1758–64.
27. Jin G, Howe PH. Regulation of clusterin gene expression by transforming growth factor β. J Biol Chem 1997;272:26620–6.
28. Bierie B, Moses HL. Tumour microenvironment: TGFβ: the molecular Jekyll and Hyde of cancer. Nat Rev Cancer 2006;6:506–20.
29. Massague J. TGFβ in cancer. Cell 2008;134:215–30.
30. Volinia S, Calin GA, Liu CG, et al. A microRNA expression signature of human solid tumors defines cancer gene targets. Proc Natl Acad Sci U S A 2006;103:2257–61.
31. Markowitz S, Wang J, Myeroff L, et al. Inactivation of the type II TGF-β receptor in colon cancer cells with microsatellite instability. Science 1995;268:1336–8.
32. Schwarte-Waldhoff I, Volpert OV, Bouck NP, et al. Smad4/DPC4-mediated tumor suppression through suppression of angiogenesis. Proc Natl Acad Sci U S A 2000;97:9624–9.
33. Miranda KC, Huynh T, Tay Y, et al. A pattern-based method for the identification of MicroRNA binding sites and their corresponding heteroduplexes. Cell 2006;126:1203–17.
34. Padua D, Zhang XH, Wang Q, et al. TGFβ primes breast tumors for lung metastasis seeding through angiopoietin-like 4. Cell 2008;133:66–77.
35. Ito Y, Oike Y, Yasunaga K, et al. Inhibition of angiogenesis and vascular leakiness by angiopoietin-related protein 4. Cancer Res 2003;63:6651–7.
36. Alexandrow MG, Kawabata M, Aakre M, Moses HL. Overexpression of the c-Myc oncoprotein blocks the growth-inhibitory response but is required for the mitogenic effects of transforming growth factor β1. Proc Natl Acad Sci U S A 1995;92:3239–43.
37. Warner BJ, Blain SW, Seoane J, Massague J. Myc downregulation by transforming growth factor β required for activation of the p15 (Ink4b) G(1) arrest pathway. Mol Cell Biol 1999;19:5913–22.
38. Seoane J, Pouponnot C, Staller P, Schader M, Eilers M, Massague J. TGFβ influences Myc, Miz-1 and Smad to control the CDK inhibitor p15INK4b. Nature Cell Biol 2001;3:400–8.
39. Staller P, Peukert K, Kiermaier A, et al. Repression of p15INK4b expression by Myc through association with Miz-1. Nat Cell Biol 2001;3:392–9.
40. Amati B. Integrating Myc and TGFβ signalling in cell-cycle control. Nat Cell Biol 2001;3:E112–3.
41. Feng XH, Liang YY, Liang M, Zhai W, Lin X. Direct interaction of c-Myc with Smad2 and Smad3 to inhibit TGF-β-mediated induction of the CDK inhibitor p15(Ink4B). Mol Cell 2002;9:133–43.

42. Schuhmacher M, Kohlhuber F, Holzel M, et al. The transcriptional program of a human B cell line in response to Myc. Nucleic Acids Res 2001;29:397–406.
43. Zeller KI, Jegga AG, Aronow B, O'Donnell KA, Dang CV. An integrated database of genes responsive to the Myc oncogenic transcription factor: identification of direct genomic targets. Genome Biol 2003;4: R69.1–R69.10.
44. Gregory PA, Bert AG, Paterson EL, et al. The miR-200 family and miR-205 regulate epithelial to mesenchymal transition by targeting ZEB1 and SIP1. Nat Cell Biol 2008;10:593–601.
45. Park SM, Gaur AB, Lengyel E, Peter ME. The miR-200 family determines the epithelial phenotype of cancer cells by targeting the E-cadherin repressors ZEB1 and ZEB2. Genes Dev 2008;22:894–907.
46. Fontana L, Fiori ME, Albini S, et al. Antagomir-17–5p abolishes the growth of therapy-resistant neuroblastoma through p21 and BIM. PLoS One 2008;3:e2236.
47. Ventura A, Young AG, Winslow MM, et al. Targeted deletion reveals essential and overlapping functions of the miR-17 through 92 family of miRNA clusters. Cell 2008;132:875–86.
48. Koralov SB, Muljo SA, Galler GR, et al. Dicer ablation affects antibody diversity and cell survival in the B lymphocyte lineage. Cell 2008;132:860–74.
49. Xiao C, Srinivasan L, Calado DP, et al. Lymphoproliferative disease and autoimmunity in mice with increased miR-17-92 expression in lymphocytes. Nat Immunol 2008;9:405–14.
50. Mavrakis KJ, Wolfe AL, Oricchio E, et al. Genome-wide RNA-mediated interference screen identifies miR-19 targets in Notch-induced T-cell acute lymphoblastic leukaemia. Nat Cell Biol 2010;12:372–9.
51. Inomata M, Tagawa H, Guo YM, Kameoka Y, Takahashi N, Sawada K. MicroRNA-17-92 down-regulates expression of distinct targets in different B-cell lymphoma subtypes. Blood 2009;113:396–402.
52. Davis BN, Hilyard AC, Lagna G, Hata A. SMAD proteins control DROSHA-mediated microRNA maturation. Nature 2008;454:56–61.
53. Petrocca F, Vecchione A, Croce CM. Emerging role of miR-106b-25/miR-17-92 clusters in the control of transforming growth factor β signaling. Cancer Res 2008;68:8191–4.
54. Rai D, Kim SW, McKeller MR, Dahia PL, Aguiar RC. Targeting of SMAD5 links microRNA-155 to the TGF-β pathway and lymphomagenesis. Proc Natl Acad Sci U S A 2010;107:3111–6.
55. Rogler CE, Levoci L, Ader T, et al. MicroRNA-23b cluster microRNAs regulate transforming growth factor-β/bone morphogenetic protein signaling and liver stem cell differentiation by targeting Smads. Hepatology 2009;50:575–84.
56. Diosdado B, van de Wiel MA, Terhaar Sive Droste JS, et al. MiR-17-92 cluster is associated with 13q gain and c-myc expression during colorectal adenoma to adenocarcinoma progression. Br J Cancer 2009;101:707–14.
57. He L, Thomson JM, Hemann MT, et al. A microRNA polycistron as a potential human oncogene. Nature 2005;435:828–33.
58. Olive V, Bennett MJ, Walker JC, et al. miR-19 is a key oncogenic component of mir-17-92. Genes Dev 2009;23:2839–49.
59. Mu P, Han YC, Betel D, et al. Genetic dissection of the miR-17~92 cluster of microRNAs in Myc-induced B-cell lymphomas. Genes Dev 2009;23:2806–11.
60. Fontana L, Pelosi E, Greco P, et al. MicroRNAs 17-5-20a-106a control monocytopoiesis through AML1 targeting and M-CSF receptor upregulation. Nat Cell Biol 2007;9:775–87.
61. Schulte JH, Horn S, Otto T, et al. MYCN regulates oncogenic microRNAs in neuroblastoma. Int J Cancer 2008;122:699–704.
62. Northcott PA, Fernandez L, Hagan JP, et al. The miR-17/92 polycistron is up-regulated in sonic hedgehog-driven medulloblastomas and induced by N-myc in sonic hedgehog-treated cerebellar neural precursors. Cancer Res 2009;69:3249–55.
63. Hellebrekers DM, Melotte V, Vire E, et al. Identification of epigenetically silenced genes in tumor endothelial cells. Cancer Res 2007;67: 4138–48.